The β1 Subunit Enhances Oxidative Regulation of Large-Conductance Calcium-activated K^+ Channels

Lindsey Ciali Santarelli,[1] Jianguo Chen,[2] Stefan H. Heinemann,[3] and Toshinori Hoshi[1]

[1]Neuroscience Graduate Group and Department of Physiology, School of Medicine, University of Pennsylvania, Philadelphia, PA 19104
[2]Department of Pharmacology, Tongji Medical College, Huazhong University of Science and Technology, Wuhan, 430030, China
[3]Molecular and Cellular Biophysics, Medical Faculty of the Friedrich Schiller University Jena, D-07747 Jena, Germany

abstract Oxidative stress may alter the functions of many proteins including the Slo1 large conductance calcium-activated potassium channel (BK_{Ca}). Previous results demonstrated that in the virtual absence of Ca^{2+}, the oxidant chloramine-T (Ch-T), without the involvement of cysteine oxidation, increases the open probability and slows the deactivation of BK_{Ca} channels formed by human Slo1 (*h*Slo1) α subunits alone. Because native BK_{Ca} channel complexes may include the auxiliary subunit β1, we investigated whether β1 influences the oxidative regulation of *h*Slo1. Oxidation by Ch-T with β1 present shifted the half-activation voltage much further in the hyperpolarizing direction (−75 mV) as compared with that with α alone (−30 mV). This shift was eliminated in the presence of high $[Ca^{2+}]_i$, but the increase in open probability in the virtual absence of Ca^{2+} remained significant at physiologically relevant voltages. Furthermore, the slowing of channel deactivation after oxidation was even more dramatic in the presence of β1. Oxidation of cysteine and methionine residues within β1 was not involved in these potentiated effects because expression of mutant β1 subunits lacking cysteine or methionine residues produced results similar to those with wild-type β1. Unlike the results with α alone, oxidation by Ch-T caused a significant acceleration of channel activation only when β1 was present. The β1 M177 mutation disrupted normal channel activation and prevented the Ch-T–induced acceleration of activation. Overall, the functional effects of oxidation of the *h*Slo1 pore-forming α subunit are greatly amplified by the presence of β1, which leads to the additional increase in channel open probability and the slowing of deactivation. Furthermore, M177 within β1 is a critical structural determinant of channel activation and oxidative sensitivity. Together, the oxidized BK_{Ca} channel complex with β1 has a considerable chance of being open within the physiological voltage range even at low $[Ca^{2+}]_i$.

key words: BK_{Ca} • *h*Slo • chloramine-T • methionine • cysteine

INTRODUCTION

The large conductance calcium-activated potassium channel (BK_{Ca}) exists in various types of cells and tissues including smooth muscle and brain. In response to depolarization and/or a rise in intracellular Ca^{2+} ($[Ca^{2+}]_i$), BK_{Ca} channels mediate net K^+ efflux to repolarize the membrane potential to the resting state. This function serves an important role in muscle contraction—during which Ca^{2+} sparks activate the BK_{Ca} channels leading to vasorelaxation (Nelson et al., 1995; Jaggar et al., 2000)—and the afterhyperpolarization phase of the action potential in select neurons (Storm, 1987). Furthermore, the impairments exhibited by mice lacking the channel indicate that BK_{Ca} channels influence normal urinary bladder (Meredith et al., 2004) and cerebellar functions (Sausbier et al., 2004).

The human BK_{Ca} channel pore-forming α subunit (*h*Slo1) contains seven putative transmembrane-spanning regions (Dworetzky et al., 1994; Pallanck and Ganetzky, 1994; Tseng-Crank et al., 1994). The S0 transmembrane domain, which distinguishes the *Slo* from the *Shaker* family of voltage-dependent potassium channels, is thought to be a site of interaction with auxiliary β subunits (Wallner et al., 1996; Meera et al., 1997). Multiple types of β subunits (β1–4) have been isolated in mammals, each with a different tissue distribution and function (Knaus et al., 1994; Xia et al., 1999; Brenner et al., 2000a; Uebele et al., 2000).

The β1 subunit is a 25-kD membrane protein consisting of two transmembrane domains connected by a large extracellular loop, such that both the NH_2 and COOH termini are intracellularly located (Knaus et al., 1994; Orio et al., 2002; Patterson et al., 2002). The β1 subunit is present in the brain, particularly in the hippocampus

Address correspondence to Toshinori Hoshi, Dept. of Physiology, University of Pennsylvania, 3700 Hamilton Walk, Philadelphia, PA 19104-6085. Fax: (215) 573-5851; email: hoshi@hoshi.org.

Abbreviations used in this paper: BK_{Ca} channel, large conductance calcium-activated potassium channel; Ch-T, chloramine-T; ΔG_{Ca}, change in free energy change associated with Ca^{2+} binding; met-O, methionine sulfoxide; Q_{app}, apparent equivalent charge movement; ROS/RNS, reactive oxygen/nitrogen species; $V_{0.5}$, half-activation voltage; z, equivalent charge.

J. Gen. Physiol. © The Rockefeller University Press • 0022-1295/2004/10/357/14 $8.00
Volume 124 October 2004 357–370
http://www.jgp.org/cgi/doi/10.1085/jgp.200409144

The Journal of General Physiology

and corpus callosum (Tseng-Crank et al., 1996), but is predominantly expressed in smooth muscle (Garcia-Calvo et al., 1994; Tanaka et al., 1997). The impaired vasorelaxation found in β1 knockout mice (Brenner et al., 2000b; Pluger et al., 2000) and the down-regulation of β1 expression associated with some forms of hypertension (Gollasch et al., 2002; Amberg et al., 2003; Amberg and Santana, 2003) clearly underscore the important physiological role of β1 in the BK_{Ca} channel regulation of vascular function. The presence of β1 modulates BK_{Ca} channel activity by enhancing the apparent Ca^{2+} sensitivity of the pore-forming subunit and also by slowing the activation/deactivation kinetics, even in the virtual absence of Ca^{2+} (McManus et al., 1995; Wallner et al., 1995; Meera et al., 1996; Nimigean and Magleby, 1999, 2000; Cox and Aldrich, 2000; Qian and Magleby, 2003). The structural determinants within β1 responsible for these critical modulatory properties are just beginning to be identified (Fernandez-Fernandez et al., 2004).

Other regulatory mechanisms such as phosphorylation, pH, and the cellular redox state influence BK_{Ca} channel activity (Weiger et al., 2002). During oxidative stress, cellular reactive oxygen/nitrogen species (ROS/RNS) readily modify cysteine and methionine residues in proteins. Oxidation of cysteine typically leads to the formation of disulfides, whereas oxidation of methionine residues creates the polar methionine sulfoxide (met-O). Oxidative modifications of amino acids differentially influence BK_{Ca} channel function depending on the ROS/RNS, the residues modified within the channel, as well as the experimental model system (DiChiara and Reinhart, 1997; Sobey et al., 1997; Wang and Wu, 1997; Wang et al., 1997; Barlow et al., 2000; Gong et al., 2000; Soh et al., 2001; Brakemeier et al., 2003). Studies using heterologously expressed *h*Slo1 indicate that oxidation of cysteine residues typically decreases the channel open probability (DiChiara and Reinhart, 1997; Soto et al., 2002; Tang et al., 2004). In contrast, methionine oxidation of the *h*Slo1 pore-forming subunit that is promoted by the oxidant chloramine-T (Ch-T) increases the channel open probability (Tang et al., 2001).

Oxidative stress is prominently involved in many disease states such as vascular dysfunction (Taniyama and Griendling, 2003) and neurodegenerative diseases (Knight, 1997; Markesbery, 1997; Butterfield et al., 2001). These physiological systems that are affected by oxidative stress depend on BK_{Ca} channel activity for normal function. Therefore, determining the effect of oxidative modification of BK_{Ca} channel complexes that closely resemble native channels is important to understand and possibly treat or prevent these diseases. Native BK_{Ca} channels are often multi-subunit complexes containing both Slo1 and auxiliary β subunits (Garcia-Calvo et al., 1994; Knaus et al., 1994; Giangiacomo et al., 1995; Vogalis et al., 1996; Tanaka et al., 1997; Wanner et al., 1999; Weiger et al., 2000). However, the influence of β subunits on the oxidative regulation of Slo1 function has not been thoroughly examined.

The purpose of the present work was to determine whether the presence of β1 alters the functional effects of *h*Slo1 oxidation. Methionine oxidation of *h*Slo1 alone causes a shift in the macroscopic G-V curve by −30 mV and slows deactivation without any appreciable effect on the activation kinetics at depolarized voltages (Tang et al., 2001). We show that, in the virtual absence of Ca^{2+}, the auxiliary subunit β1 dramatically potentiates the effect of methionine oxidation in the *h*Slo1 pore-forming protein. This is demonstrated by a further increase in the open probability and even greater slowing of the deactivation kinetics. Furthermore, β1 confers novel oxidation sensitivity to the channel activation kinetics that is mediated largely by a single methionine residue located in the second transmembrane domain (TM2) of β1.

MATERIALS AND METHODS

Channel Expression and Mutagenesis

*h*Slo1 (U11058, hbr1; Tseng-Crank et al., 1994) channel alone, or *h*Slo1 and β1 (1:1 weight ratio) were transiently expressed in HEK-tsA cells using FuGENE 6 (Roche Applied Science) as described previously (Avdonin et al., 2003). The mouse Slo β1 (*m*β1; AF020711; Jiang et al., 1999) in pEGFP-N1 (BD Biosciences) was obtained from the laboratory of R. Aldrich (Stanford University, Stanford, CA). The *m*β1 mutants M7L, M23L, M177L, and Triple (M7L:M23L:M177L) were constructed using PCR-based mutagenesis, and the sequences were verified. "Cys-less" *b*β1, in which every cysteine in bovine β1 (*b*β1; L26101; Knaus et al., 1994) was replaced with alanine (C18A, C53A, C76A, C103A, and C135A; Hanner et al., 1998), was obtained from the laboratory of M.L. Garcia (Merck Research Laboratories, Rahway, NJ).

Electrophysiology and Data Analysis

Currents were recorded from excised inside-out patches at room temperature essentially as described previously (Tang et al., 2001). Patch electrodes (Warner) had a typical initial resistance of 2.5–3 MΩ when filled with solutions (described in the next section); the series resistance, ∼90% of the input resistance, was electronically compensated. The current signal was filtered at 10 kHz through the built-in filter of the patch-clamp amplifier (model AxoPatch 200A; Axon Instruments). Data were acquired and analyzed using Pulse/PulseFit (HEKA), PatchMachine (Avdonin et al., 2003), and IgorPro (WaveMetrics) as described for single-channel data (Avdonin and Hoshi, 2001) and macroscopic current data (Tang et al., 2001; Avdonin et al., 2003). In brief, normalized macroscopic conductance was estimated from single exponential fits to the tail currents recorded at −50 mV excluding the initial 180 μs after pulses to different voltages from the holding voltage of 0 mV. The apparent equivalent charge movement (Q_{app}) was derived from the simple Boltzmann function

used to describe the average G-V curve. Activation and deactivation time courses were fitted by single exponentials excluding the initial 150- and 180-μs segments, respectively. A single exponential fit to the voltage dependence of the time constant provided the value of the equivalent charge movement (z).

In some patches, the tail currents after Ch-T treatment contained a minor fast component. The fractional amplitude of this component was typically small (<10%), and the time constant estimated from single-exponential fits was essentially the same as that of the slow component estimated from two-exponential fits. Thus, single-exponential fits were used throughout to quantify the tail current kinetics. Because the time constant of the tail current before modification and that of the minor fast component after Ch-T treatment were similar, the fast component likely reflects the kinetics of unmodified channels.

The change in free energy associated with Ca^{2+} binding (ΔG_{Ca}) was determined based on the ΔG_{Ca} contribution to channel open probability (P_O) as described previously (Tang et al., 2004). The values of P_O, ΔG_o, ΔG_V, and ΔG_{Ca} were estimated by fitting the G-V curves obtained in 0 and 2.1 μM Ca^{2+}.

Statistical comparisons were made using the paired t test. In some cases, the t test and ANOVA followed by the Bonferroni post hoc test were used as specifically indicated (DataDesk; Data Description). Statistical significance was assumed at $P \leq 0.05$. Where appropriate, data are presented as mean ± SEM.

Reagents and Solutions

Both the external and internal recording solutions contained the following (mM): 140 KCl, 11 EGTA, and 10 HEPES, pH 7.2 adjusted with NMDG. The free Ca^{2+} concentration for these solutions was estimated at <1 nM assuming 20 μM contaminating Ca^{2+} (Patcher's Power Tools v1.0, F. Mendez; http://www.mpibpc.gwdg.de/abteilungen/140/software/). The external solution used to reduce the size of inward K^+ currents for experiments involving 2.1 μM $[Ca^{2+}]_i$ contained the following (mM): 70 KCl, 70 NaCl, 2 $MgCl_2$, and 10 HEPES, pH 7.2 adjusted with NMDG. The 2.1-μM free Ca^{2+} internal solution contained the following (mM): 120 KCl, 20 KOH, 1 $MgCl_2$, 2.2 $CaCl_2$, 4 HEDTA, and 10 HEPES, pH 7.4 adjusted with NMDG. The external solution used for experiments involving 120 μM $[Ca^{2+}]_i$ contained the following reagents (mM): 140 KCl, 2 $MgCl_2$, and 10 HEPES, pH 7.2 adjusted with NMDG. The 120-μM free Ca^{2+} internal solution contained the following reagents (mM): 140 KCl, 10 $MgCl_2$, 0.1 $CaCl_2$, and 10 HEPES, pH 7.2 adjusted with NMDG.

Chloramine-T (Ch-T; Sigma-Aldrich) was dissolved in the internal solution immediately before use. In every experiment, 2 mM Ch-T was manually applied with a pipette to ensure the addition of six times the bath volume (∼150 μl). With Ch-T present, channel current in response to a pulse to 120 mV was monitored every 5 s for the following three features of oxidation by Ch-T: increased current amplitude, slowed deactivation, and accelerated activation. Once these characteristic changes reached steady-state levels (≤8 min), Ch-T was subsequently washed out with 1 ml of recording solution. The time courses of modification of channels, composed of either *h*Slo1 alone or *h*Slo1 and β1 together, were indistinguishable.

RESULTS

Oxidation by Ch-T More Dramatically Enhances hSlo1 Currents When β1 Is Present

To determine if the presence of β1 influences the functional effects of *h*Slo1 oxidation by Ch-T, ionic currents through *h*Slo1 or *h*Slo1 + *m*β1 channels were recorded in the inside-out patch-clamp configuration from transiently transfected HEK-tsA cells. All recordings were initially made in the virtual absence of Ca^{2+}, essentially permitting the Slo channel to act as a voltage-dependent channel to simplify the data analysis (Meera et al., 1996; Horrigan and Aldrich, 1999; Horrigan et al., 1999). Currents elicited by pulses to 120 mV in patches containing either *h*Slo1 or *h*Slo1 + *m*β1 are shown in Fig. 1 A (thin sweeps). The *h*Slo1 + *m*β1 currents displayed slow activation and deactivation (also see Fig. 2), a hallmark of the functional presence of the β1 subunit. After bath application of 2 mM Ch-T to the cytoplasmic side, *h*Slo1 and *h*Slo1 + *m*β1 exhibited similar modification time courses ($P = 0.08$, t test) that resulted in larger current amplitudes (Fig. 1 A, thick sweeps). The current enhancement remained after Ch-T washout, consistent with the oxidative modification of the channel protein complex by Ch-T.

Treatment with Ch-T shifted the peak I-V curves from both *h*Slo1 and *h*Slo1 + *m*β1 to more negative voltages, such that at a given voltage, the current size was greater (Fig. 1 B). However, the current enhancement was drastically larger in *h*Slo1 + *m*β1 than in *h*Slo1 alone, especially at moderately depolarizing voltages (50–100 mV; Fig. 1 B). The relative increase in current amplitude due to oxidation became progressively smaller at more depolarizing voltages where the channel open probability is saturated. This voltage dependence is consistent with Ch-T increasing the open channel probability as shown for *h*Slo1 (Tang et al., 2001).

The voltage dependence of the probability of the channel being open inferred from normalized macroscopic G-V curves confirmed that treatment with Ch-T enhanced the open probability of *h*Slo1 + *m*β1 more profoundly than that of *h*Slo1 alone. The G-V curves estimated from tail current measurements were fit by a simple Boltzmann function as a data descriptor to describe the overall voltage dependence of the Ch-T effect (Fig. 1 C). After Ch-T treatment, the *h*Slo1 half-activation voltage ($V_{0.5}$) shifted by ∼30 mV in the hyperpolarizing direction. However, for *h*Slo1 + *m*β1, oxidation by Ch-T produced the strikingly greater shift of −75 mV. The mean shift in $V_{0.5}$ for *h*Slo1 + *m*β1 ($\Delta V_{0.5} = -74.6 \pm 3.5$ mV, $n = 14$) was more than twice as great as $\Delta V_{0.5}$ for *h*Slo1 alone ($\Delta V_{0.5} = -31.3 \pm 3.3$ mV, $n = 7$) (Fig. 1 D; $P < 0.0001$, t test). These results suggest that treatment with Ch-T leads to an increase in the open probability that is markedly potentiated with *m*β1 present.

The apparent equivalent charge movement (Q_{app}) of *h*Slo1 activation, inferred from the steepness of the G-V curve, decreased by ∼23% ($\Delta Q_{app} = -0.25 \pm 0.07e$, $P = 0.036$, $n = 7$) after Ch-T treatment (Fig. 1 D). In contrast, the ΔQ_{app} for *h*Slo1 + *m*β1 demonstrated no significant change after modification ($\Delta Q_{app} = 0.02 \pm 0.02e$; $P = 0.65$, $n = 14$).

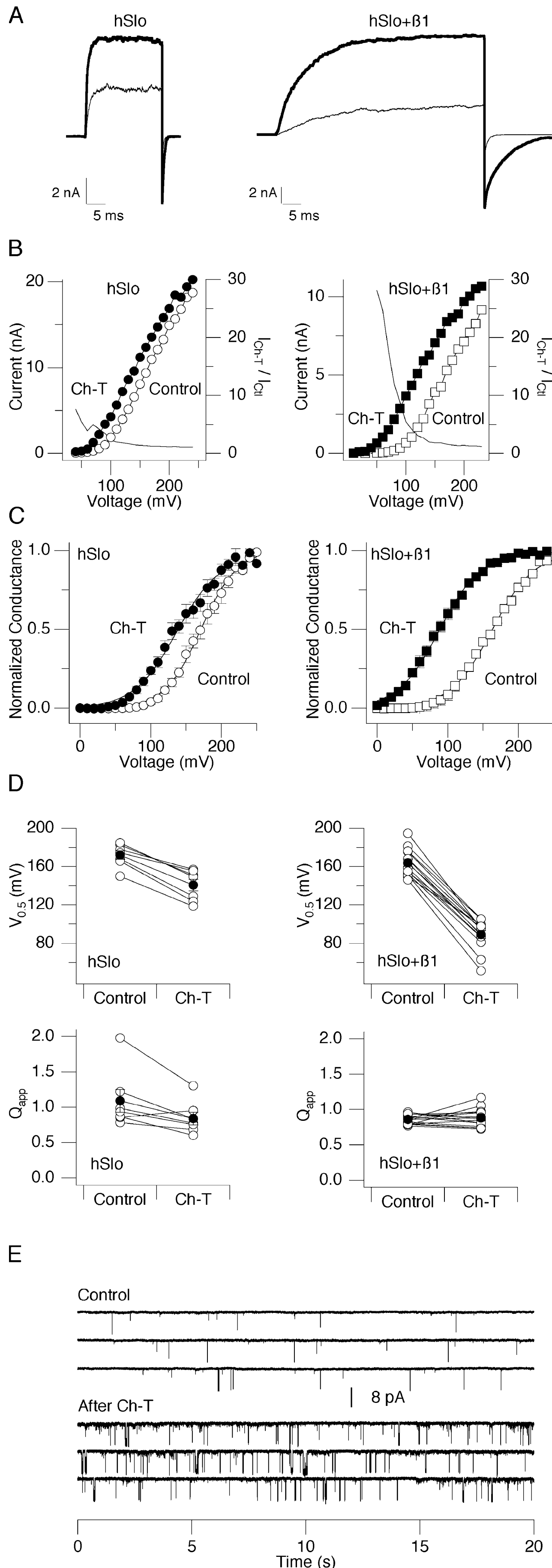

The increase in the channel open probability caused by Ch-T was maintained at more negative, physiological voltages. At −40 mV in the virtual absence of Ca^{2+}, treatment with Ch-T markedly increased the number of *h*Slo1 + *m*β1 channel openings (Fig. 1 E). Indeed, the mean open probability at this voltage increased by a factor of 12.0 ± 3.0 relative to control. In contrast with the dramatic changes in the gating properties of the *h*Slo1 + *m*β1 channel, the open channel current-conductance characteristic estimated using voltage ramps (0–250 mV) in single-channel patches remained unaltered by Ch-T treatment (unpublished data).

Modification by Ch-T Drastically Slows hSlo1 + mβ1 Deactivation

To assess whether treatment with Ch-T affects *h*Slo1 deactivation differently when the β1 subunit is present, *h*Slo1 and *h*Slo1 + *m*β1 tail currents were recorded before and after Ch-T treatment (Fig. 2 A). After Ch-T exposure, the mean deactivation time constant at −40 mV increased by ∼70% (from 0.26 to 0.45 ms) for *h*Slo1, whereas the increase for *h*Slo1 + *m*β1 was ∼180% (from 2.12 to 6.06 ms). This appreciably greater slowing of *h*Slo1 + *m*β1 deactivation was observed at every voltage examined (Fig. 2 B). Single exponential fits to the voltage dependence of the deactivation time constants in the voltage range of −150 to −50 mV indicated that oxidation by Ch-T specifically increased the time constant values at 0 mV, τ(0), for *h*Slo1 and *h*Slo1 + *m*β1 (P = 0.0021 and 0.015, respec-

FIGURE 1. Oxidation by Ch-T enhances *h*Slo1 + *m*β1 currents to a greater extent than *h*Slo1 currents. (A) Representative currents before (thin sweep) and after (thick sweep) 2 mM Ch-T treatment. The currents were elicited in response to pulses from 0 to 120 mV. Mean times to reach 50% of final current amplitude in the presence of Ch-T for *h*Slo1 and *h*Slo1 + *m*β1 were 5.64 ± 0.34 min and 4.68 ± 0.3 min, respectively (P = 0.08, *n* = 4). (B) Peak I-V curves before (open symbols) and after (closed symbols) modification by Ch-T. Continuous curves represent relative increases in current amplitude as a function of voltage (right axis). (C) G-V curves before (open symbols) and after (closed symbols) modification by Ch-T. The macroscopic currents were elicited by pulses to different test voltages from the holding voltage of 0 mV. The *h*Slo1 $V_{0.5}$ values for the results obtained before and after Ch-T application were 171.9 ± 4.5 mV and 140.6 ± 6.1 mV ($\Delta V_{0.5}$ range, −19 to −42 mV; P < 0.0001, *n* = 7), respectively. The *h*Slo1 + *m*β1 $V_{0.5}$ values for the results obtained before and after Ch-T application were 163.8 ± 3.8 mV and 89.2 ± 4.1 mV ($\Delta V_{0.5}$ range −50 to −99 mV; P < 0.0001, *n* = 14), respectively. The *h*Slo1 Q_{app} values for the results obtained before and after Ch-T application were 1.09 ± 0.16*e* and 0.84 ± 0.09*e* (P = 0.036, *n* = 7), respectively. The *h*Slo1 + *m*β1 Q_{app} values for the results obtained before and after Ch-T application were 0.86 ± 0.02*e* and 0.88 ± 0.04*e*, respectively, (P = 0.65, *n* = 14). (D) $V_{0.5}$ and Q_{app} values before and after oxidation by Ch-T from individual experiments (open circles) and mean values (closed circles). (E) Representative *h*Slo1 + *m*β1 channel openings at −40 mV before and after treatment with Ch-T. Data were filtered at 10 kHz and sampled at 83 kHz, but are shown filtered at 1 kHz for display purpose. Typically, 3-min segments were analyzed in each condition.

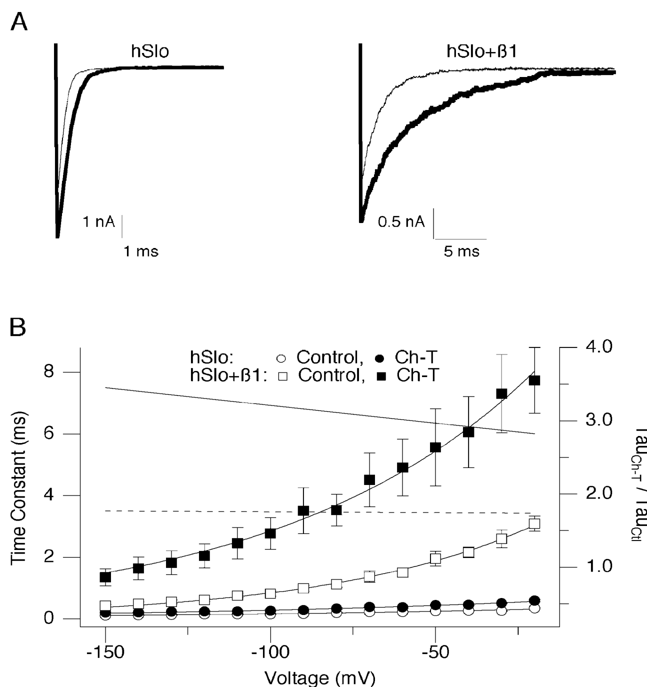

FIGURE 2. Ch-T treatment slows deactivation of *h*Slo1 + *m*β1 to a greater extent than *h*Slo1 deactivation. (A) Tail currents recorded at −40 mV after pulses to 180 mV before (thin sweep) and after (thick sweep) Ch-T treatment. (B) Voltage dependence of the deactivation time constant for *h*Slo1 control (open circles; *n* = 7), *h*Slo1 after Ch-T (closed circles; *n* = 7), *h*Slo1 + *m*β1 control (open squares; *n* = 5), and *h*Slo1 + *m*β1 after Ch-T (closed squares; *n* = 5). The *h*Slo1 τ(0) and *z* values obtained before and after Ch-T application were 0.35 ± 0.04 ms and 0.19 ± 0.01*e*, and 0.63 ± 0.06 ms and 0.21 ± 0.01*e*, respectively. The *h*Slo1 + *m*β1 τ(0) and *z* values obtained before and after Ch-T application were 3.96 ± 0.52 ms and 0.38 ± 0.02*e*, and 10.9 ± 2.1 ms and 0.34 ± 0.01*e*, respectively. The relative increase in the value of the deactivation time constant as a function of voltage (right axis) is shown for *h*Slo1 (dashed line) and *h*Slo1 + *m*β1 (continuous line).

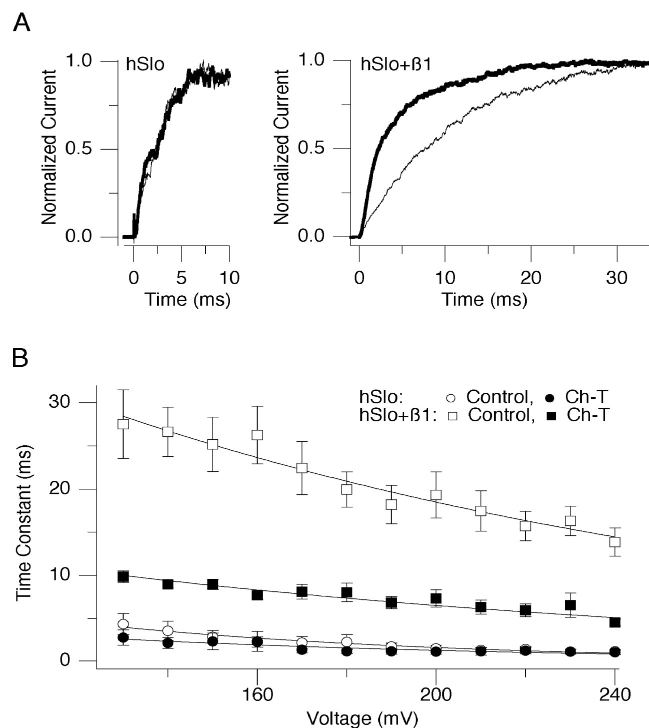

FIGURE 3. Modification by Ch-T accelerates activation of *h*Slo1 + *m*β1. (A) Normalized currents recorded at 240 mV from the holding voltage of 0 mV before (thin sweep) and after (thick sweep) Ch-T treatment. (B) Voltage dependence of the activation time constant for *h*Slo1 control (open circles; *n* = 7), *h*Slo1 after Ch-T (closed circles; *n* = 7), *h*Slo1 + *m*β1 control (open squares; *n* = 14), and *h*Slo1 + *m*β1 after Ch-T (closed squares; 5 ≤ *n* ≤ 12). The *h*Slo1 τ(0) and *z* values obtained before and after Ch-T application were 7.0 ± 1.2 ms and 0.28 ± 0.05*e*, and 4.4 ± 1.0 ms and 0.22 ± 0.02*e*, respectively. The *h*Slo1 + *m*β1 τ(0) and *z* values obtained before and after Ch-T application were 0.082 ± 0.01 s and 0.171 ± 0.02*e*, and 0.026 ± 0.003 s and 0.174 ± 0.02*e*, respectively.

tively, *n* = 5) without significantly affecting their equivalent charge movement (P = 0.17 and 0.08, respectively, *n* = 5). In fact, the change in τ(0) for *h*Slo1 + *m*β1 is approximated by a voltage shift of −75 mV, which is similar in value to the voltage shift of the G-V curve after oxidation by Ch-T.

Activation Kinetics of hSlo1 + mβ1 Accelerates after Ch-T Treatment

The activation kinetics of *h*Slo1 alone remained unaltered after modification by Ch-T (Fig. 3 A; Tang et al., 2001). In contrast, Ch-T markedly accelerated the mean activation kinetics of *h*Slo1 + *m*β1 by 68% at each voltage tested (130–240 mV; Fig. 3 B). Single exponential fits to the voltage dependence of the activation time constant within this voltage range demonstrated that treatment with Ch-T decreased τ(0) for *h*Slo1 + *m*β1 (P = 0.002, *n* = 7), but not for *h*Slo1 (P = 0.23, *n* = 4), without affecting the equivalent charge movement (*h*Slo1: P = 0.14, *n* = 4; *h*Slo1 + *m*β1: P = 0.92, *n* = 7). This change in τ(0) could be accounted for by a voltage shift of more than −150 mV, which is much larger in value than the voltage shift of the G-V curve after oxidation by Ch-T.

Altogether, modification by Ch-T caused a much greater increase in *h*Slo1 open probability, an enhanced slowing of deactivation, and a distinct acceleration of activation kinetics when β1 was coexpressed. These Ch-T–induced changes specific to *h*Slo1 + *m*β1 may involve any of the following possible mechanisms. First, given that cysteine residues are also potential targets of Ch-T under physiological conditions, oxidation of cysteine within β1 may account for the enhanced oxidative regulation of *h*Slo1 + *m*β1. Second, oxidation of methionine within β1 may synergistically enhance the functional effects of *h*Slo1 oxidation. Third, the mere presence of β1 may potentiate the functional outcome of oxidation within the *h*Slo1 pore-forming subunit. These possible mechanisms are addressed in the next sections.

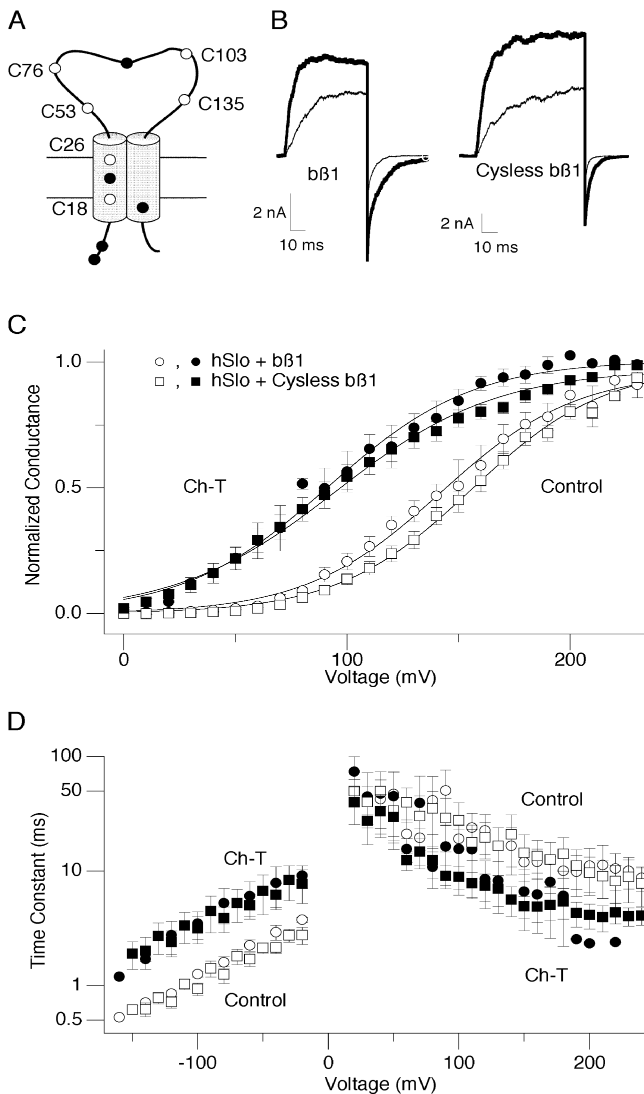

FIGURE 4. Cysless $b\beta1$ resembles wild-type $b\beta1$. (A) A schematic representation of cysteine residues (open circles) in $m\beta1$. C26 does not exist in $b\beta1$. Closed circles represent methionine residues. (B) Representative currents before (thin sweep) and after (thick sweep) Ch-T treatment. The currents were elicited in response to pulses from 0 to 140 mV. (C) G-V curves before and after modification by Ch-T. The *h*Slo1 + $b\beta1$ $V_{0.5}$ values for the results obtained before (open circles) and after (closed circles) Ch-T application were 145.5 ± 8.2 mV and 91.4 ± 9.6 mV ($\Delta V_{0.5}$ range, −51 to −56 mV; P = 0.0009; n = 3), respectively. The *h*Slo1 + Cysless $b\beta1$ $V_{0.5}$ values for the results obtained before (open squares) and after (closed squares) Ch-T application were 156.6 ± 4.5 mV and 98.5 ± 7.4 mV ($\Delta V_{0.5}$ range, −39 to −77 mV; P < 0.0001, n = 10), respectively. The *h*Slo1 + $b\beta1$ Q_{app} values for the results obtained before and after Ch-T application were 0.82 ± 0.06*e* and 0.8 ± 0.04*e* (P = 0.8, n = 3), respectively. The *h*Slo1 + Cysless $b\beta1$ Q_{app} values for the results obtained before and after Ch-T application were 0.88 ± 0.03*e* and 0.74 ± 0.05*e*, respectively (P = 0.009, n = 10). (D) Voltage dependence of the deactivation and activation time constants. Symbols are the same as in C.

Cysless β1 Produces Results Similar to Wild-type β1

Previous results demonstrated that cysteine modification within *h*Slo1 is not involved in the Ch-T–mediated response (Tang et al., 2001). To test whether the enhanced effects of Ch-T on channel behavior in the presence of β1 involve modification of cysteine residues within the β1 subunit, we used a mutant $b\beta1$ subunit devoid of any cysteine named Cysless $b\beta1$ (Fig. 4 A; Hanner et al., 1998). Because this mutant was derived from bovine β1, we compared the results from *h*Slo1 + $b\beta1$ with *h*Slo1 + Cysless $b\beta1$.

Expression of Cysless $b\beta1$ slowed the *h*Slo1 activation and deactivation kinetics in the control condition essentially as observed with wild-type $b\beta1$ (Fig. 4 B), confirming that Cysless $b\beta1$ functionally interacts with *h*Slo1. Ch-T treatment enhanced the currents through both *h*Slo1 + $b\beta1$ and *h*Slo1 + Cysless $b\beta1$ in a similar manner. After modification by Ch-T, the *h*Slo1 + $b\beta1$ and *h*Slo1 + Cysless $b\beta1$ G-V curves shifted leftward (Fig. 4 C), such that the mean $\Delta V_{0.5}$ values were indistinguishable (−54.1 ± 1.7 mV and −58.1 ± 3.6 mV, n = 3 and 10, respectively). Importantly, these $\Delta V_{0.5}$ values were markedly greater than those found with *h*Slo1 alone ($\Delta V_{0.5} \approx -30$ mV; Fig. 1 D) ($P < 0.05$; Bonferroni test). The $\Delta V_{0.5}$ values of *h*Slo1 + $b\beta1$ and *h*Slo1 + Cysless $b\beta1$ were smaller than that of *h*Slo1 + $m\beta1$ ($\Delta V_{0.5} \approx -75$ mV; Fig. 1 D) probably because the control $V_{0.5}$ values before treatment with Ch-T for the $b\beta1$ channel complexes (~145 and 156 mV, respectively) were already less depolarized than that of $m\beta1$ (~164 mV); yet, all $V_{0.5}$ values after treatment with Ch-T were ~90 mV. Nevertheless, the removal of all cysteine residues within the β1 subunit still permitted the enhanced $\Delta V_{0.5}$ after modification by Ch-T. Furthermore, the activation and deactivation time courses of *h*Slo1 + Cysless $b\beta1$ before and after treatment with the oxidant resembled those of *h*Slo1 + $b\beta1$ (Fig. 4 D). Therefore, the kinetic and G-V results for *h*Slo1 + $m\beta1$, *h*Slo1 + $b\beta1$, and *h*Slo1 + Cysless $b\beta1$ are largely similar and suggest that oxidation of cysteine residues within β1 is not responsible for the enhanced oxidative regulation of *h*Slo1 in the presence of the β1 subunit.

The Greater Increase in Open Probability Does Not Depend on Methionine Oxidation within β1

The Ch-T effect on *h*Slo1 + β1 function did not involve cysteine oxidation but the oxidation of methionine residues within β1 may be responsible. Each $m\beta1$ contains five methionine residues: M1, M7, M23, M89, and M177 (Fig. 5 A); the contribution of these methionines to the enhanced shift of the G-V curve and further slowing of deactivation, as well as acceleration of the activation kinetics was assessed in the following manner. Because M1 is obligatory for normal β1 syn-

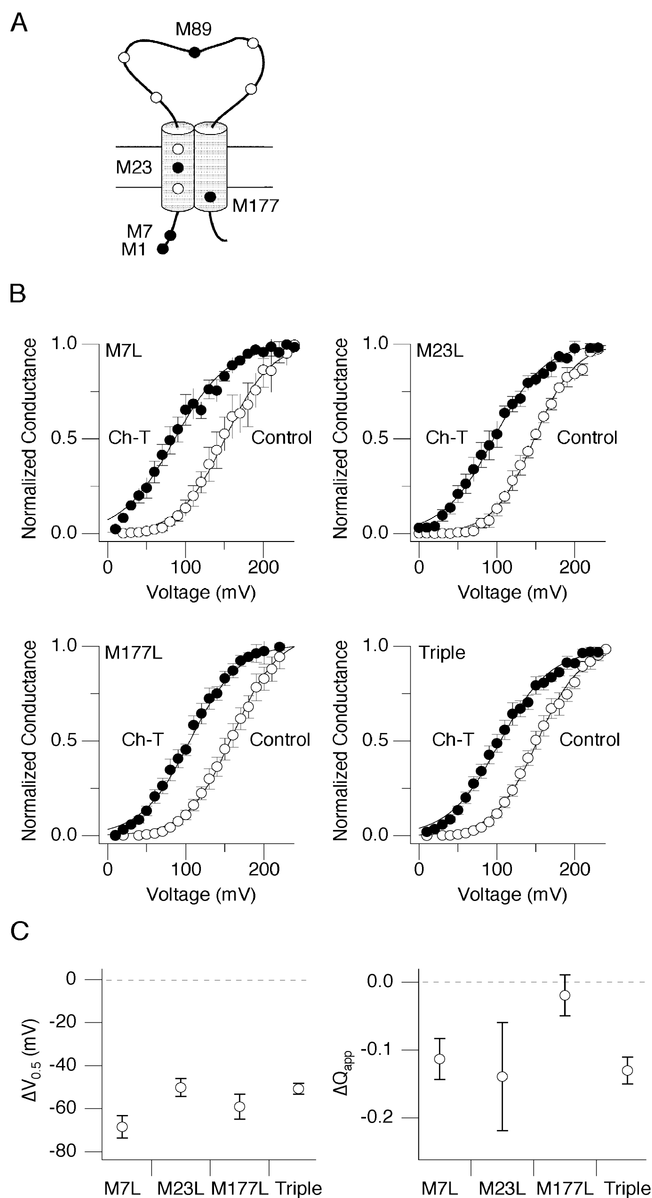

FIGURE 5. Methionine mutations within *m*β1 permit oxidation-related increases in *h*Slo1 open probability similar to wild-type *m*β1. (A) A schematic representation of methionine residues (closed circles) in *m*β1. Open circles represent cysteine residues. (B) G-V curves before and after modification by Ch-T. The *h*Slo1 + M7L, M23L, M177L, or Triple $V_{0.5}$ values for the results obtained before Ch-T application (open circles) were 153.9 ± 12.5 mV (*n* = 4), 147.1 ± 3.2 mV (*n* = 5), 164.1 ± 8.3 mV (*n* = 5), and 153.8 ± 6.2 mV (*n* = 6), respectively. After Ch-T application (closed circles), the *h*Slo1 + M7L, M23L, M177L, or Triple $V_{0.5}$ values were 85.5 ± 9 mV ($\Delta V_{0.5}$ range, −54 to −78 mV; P = 0.001, *n* = 4), 96.9 ± 6.4 mV ($\Delta V_{0.5}$ range, −42 to −60 mV; P = 0.0002, *n* = 5), 105 ± 5.9 mV ($\Delta V_{0.5}$ range, −43 to −71 mV; P = 0.0005, *n* = 5), and 103.1 ± 7.3 mV ($\Delta V_{0.5}$ range, −45 to −60 mV; P < 0.0001, *n* = 6), respectively. (C) The mean $\Delta V_{0.5}$ values (left) for *h*Slo1 + M7L, M23L, M177L, and Triple *m*β1 were −68.4 ± 5.2 mV, −50.2 ± 4.1 mV, −59.0 ± 5.8 mV, and −50.7 ± 2.6 mV, respectively. The mean ΔQ_{app} values (right) for *h*Slo1 + M7L, M23L, M177L, and Triple *m*β1 were −0.11 ± 0.03*e* (P = 0.04, *n* = 4), −0.14 ± 0.08*e* (P = 0.15, *n* = 5), −0.019 ± 0.03*e* (P = 0.6, *n* = 5), and −0.12 ± 0.04*e* (P = 0.02, *n* = 6), respectively. A negative $\Delta V_{0.5}$ indicates a leftward shift of the G-V curve, and a negative ΔQ_{app} value indicates a decrease in the slope of the G-V curve after Ch-T modification.

thesis, we could not readily test its role. M89 is present in *m*β1 but absent in *b*β1. However, both *m*β1 and *b*β1 confer to *h*Slo1 the enhanced Ch-T sensitivity, thereby excluding the critical involvement of M89 (Fig. 4). Thus, M7, M23, and M177 were individually mutated to leucine which is much less susceptible to oxidation by Ch-T than methionine (Ciorba et al., 1997). In addition, a triple *m*β1 mutant (Fig. 5, Triple) in which M7, M23, and M177 were all replaced by leucine was constructed. When coexpressed with *h*Slo1, each *m*β1 mutant channel complex exhibited currents with wild-type β1-like characteristics including slower activation and deactivation compared with *h*Slo1 alone, thus confirming that these *m*β1 mutants functionally associated with *h*Slo1.

After modification by Ch-T, each *m*β1 mutant channel complex (M7L, M23L, M177L, and Triple) showed a large leftward shift in $V_{0.5}$ (Fig. 5 B). The mean $V_{0.5}$ for *h*Slo1 + M7L, M23L, M177L, or Triple *m*β1 shifted by −68 ± 5.2 mV, −50 ± 4.1 mV, −59 ± 5.7 mV, and −50.6 ± 2.6 mV, respectively (Fig. 5 C); these $\Delta V_{0.5}$ were significantly larger than that found with *h*Slo1 alone ($\Delta V_{0.5} \approx -30$ mV; Fig. 1 D) (P < 0.05, Bonferroni test). These results indicated that oxidation of methionine residues within *m*β1 is not necessary to produce the enhanced G-V curve shift after modification by Ch-T.

Methionine Oxidation within β1 Is Not Required for the Greater Slowing of hSlo1 Deactivation

Treatment with Ch-T slowed the deactivation time course of every *h*Slo1+ mutant *m*β1 complex examined (Fig. 6 A). The extent of this slowing of *h*Slo1 deactiva-

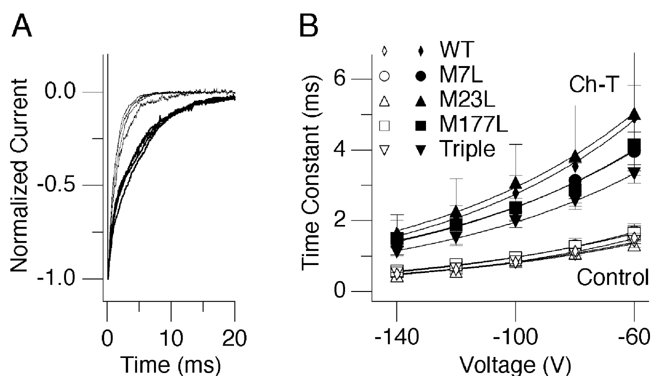

FIGURE 6. Slowing of channel deactivation after oxidation by Ch-T is maintained in all *m*β1 methionine mutant channel complexes. (A) Superimposed *h*Slo1 + M7L, M23L, M177L, or Triple *m*β1 normalized tail currents recorded at −40 mV after pulses to 180 mV before (thin sweeps) and after (thick sweeps) treatment with Ch-T. (B) Voltage dependence of the deactivation time constant for *h*Slo1 + wild type (diamonds; *n* = 5), M7L (circles; *n* = 4), M23L (triangles; *n* = 5), M177L (squares; *n* = 5), or Triple (inverted triangles; *n* = 6) *m*β1 before (open symbols) and after (closed symbols) Ch-T treatment.

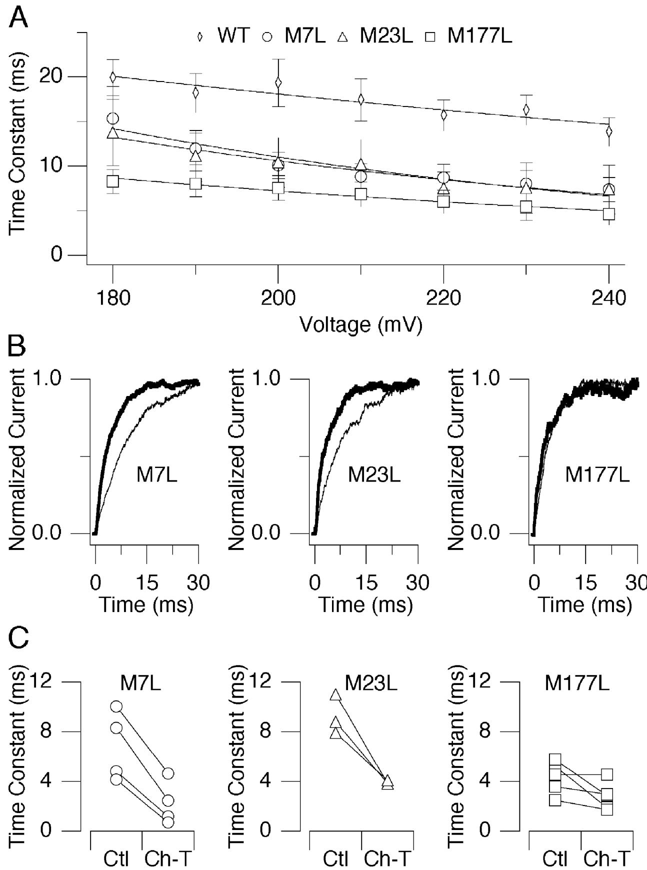

FIGURE 7. M177 in $m\beta1$ specifically affects channel activation. (A) Voltage dependence of the activation time constant before treatment with Ch-T for *h*Slo1 + wild type (diamonds; $n = 14$), M7L (circles; $n = 4$), M23L (triangles; $n = 5$), or M177L (squares; $n = 5$) $m\beta1$. (B) Currents recorded at 220 mV from the holding voltage of 0 mV before (thin sweep) and after (thick sweep) modification by Ch-T. (C) Activation time constant values at 220 mV before and after oxidation by Ch-T from individual experiments.

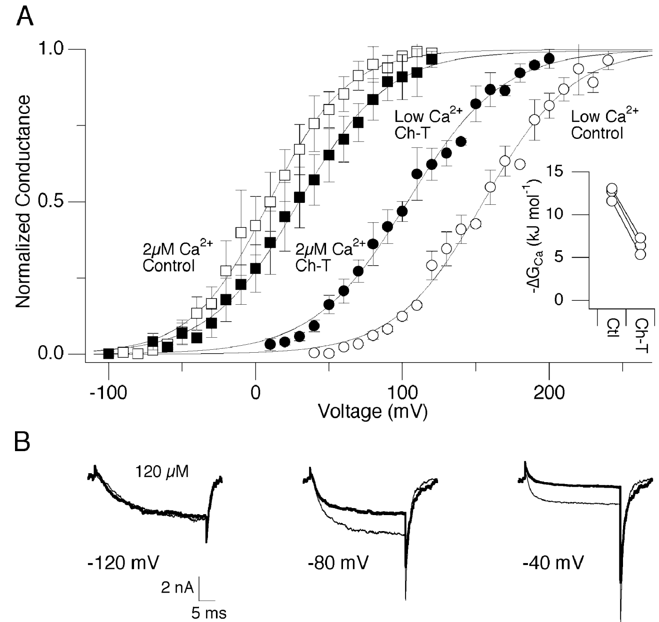

FIGURE 8. The effect of Ch-T on channel open probability depends on Ca^{2+}. (A) G-V curves before and after modification by Ch-T. Currents were first generated by pulsing to different test potentials from a holding voltage of 0 mV in the virtual absence of Ca^{2+}. This recording protocol was repeated after bath application of 2.1 μM Ca^{2+}. Tail currents were measured at −50 mV in zero $[Ca^{2+}]_i$ or −100 mV in high $[Ca^{2+}]_i$. After a return to zero Ca^{2+} for treatment with 2 mM Ch-T, the recording protocol was again repeated in zero and then 2.1 μM Ca^{2+}. The zero $[Ca^{2+}]_i$ $V_{0.5}$ values for the results obtained before (open circles) and after (closed circles) Ch-T application were 155.3 ± 5.1 mV and 103.5 ± 7.2 mV ($\Delta V_{0.5}$ range, −47 to −56 mV; P = 0.002, $n = 3$), respectively. The smaller $\Delta V_{0.5}$ value (approximately −50 vs. −75 mV; Fig. 1) was most likely because of the use of an external recording solution containing less K^+ than that previously used in the zero $[Ca^{2+}]_i$ experiments. The 2.1 μM $[Ca^{2+}]_i$ $V_{0.5}$ values for the results obtained before (open squares) and after (closed squares) Ch-T application were 9.1 ± 11.2 mV and 29.6 ± 12.5 mV ($\Delta V_{0.5}$ range, 15–25 mV; P = 0.018, $n = 3$), respectively. The zero $[Ca^{2+}]_i$ Q_{app} values for the results obtained before and after Ch-T application were 0.84 ± 0.04*e* and 0.79 ± 0.02*e* (P = 0.13, $n = 3$), respectively. The 2.1 μM $[Ca^{2+}]_i$ Q_{app} values for the results obtained before and after Ch-T application were 1.03 ± 0.07*e* and 0.88 ± 0.03*e* (P = 0.1, $n = 3$), respectively. (inset) The contribution of Ca^{2+}-dependent gating to overall channel opening (ΔG_{Ca}) before and after oxidation by Ch-T from individual experiments. (B) Representative currents from a single patch ($n = 5$) in the presence of 120 μM $[Ca^{2+}]_i$ before (thin sweeps) and after (thick sweeps) Ch-T treatment. The currents were elicited from a holding voltage of −200 mV.

tion with any of the $m\beta1$ mutants was indistinguishable from the slowing of *h*Slo1 + $m\beta1$ (Fig. 6 B). The voltage dependence of the deactivation kinetics was also unaltered by Ch-T treatment with the equivalent charge movement remaining at ~0.3*e* in all cases. Thus, the Ch-T–induced slowing of channel deactivation did not specifically require M7, M23, M177, or the presence of all three residues together in β1.

M177 in mβ1 Is Critical for Typical hSlo1 Activation Properties

Oxidative modification by Ch-T accelerated the activation kinetics of *h*Slo1 + $m\beta1$ but not of *h*Slo1 alone (Fig. 3). For channel complexes that included an $m\beta1$ methionine point mutant, there was a trend for the activation kinetics to be faster than *h*Slo1+ wild-type $m\beta1$ even before Ch-T treatment (Fig. 7 A). However, a difference in the activation time course was statistically significant only in *h*Slo1 + M177L $m\beta1$ (220 mV; P = 0.002, Bonferroni test). In fact, the activation kinetics of *h*Slo1 + M177L $m\beta1$ before Ch-T treatment was similar to that of the *h*Slo1+ wild-type $m\beta1$ complex after modification by Ch-T.

The activation kinetics of *h*Slo1 + M7L $m\beta1$ and *h*Slo1 + M23L $m\beta1$ after Ch-T treatment were significantly faster, as found with wild-type $m\beta1$ (Fig. 7, B and C; P = 0.005 and 0.03, respectively). However, Ch-T

failed to accelerate the activation time course of *h*Slo1 + M177L *m*β1 in an appreciable manner ($P \geq 0.085$). M177L *m*β1 does associate with *h*Slo1 because the deactivation kinetics of *h*Slo1 + M177L *m*β1 was indistinguishable from *h*Slo1 + *m*β1 (Fig. 6 B). Thus, M177 in TM2 of β1 is a key determinant of the activation kinetics and the oxidative sensitivity of *h*Slo1 + *m*β1.

The Effect of Ch-T Treatment with β1 Present Is Ca^{2+} Dependent

The hyperpolarizing shift in $V_{0.5}$ caused by treatment with Ch-T was essentially eliminated by increasing $[Ca^{2+}]_i$ to 2.1 μM (Fig. 8 A). Similar results were obtained with saturating levels of divalent ions, $[Ca^{2+}]_i$ = 120 μM and $[Mg^{2+}]_i$ = 10 mM (Fig. 8 B). In the presence of elevated $[Ca^{2+}]_i$, cysteine oxidation is capable of shifting the G-V curve to the right (Tang et al., 2004), which may account for the depolarizing shift seen here after treatment with Ch-T. With the assumption that the free energy changes associated with the BK_{Ca} channel intrinsic opening process, voltage-dependent activation, and Ca^{2+} binding together contribute to the overall open probability in a linearly additive manner (Cui and Aldrich, 2000), the measured G-V parameters were used to infer the free energy contributions of Ca^{2+} to channel opening (Tang et al., 2004) in the control and Ch-T treated conditions. The decrease in ΔG_{Ca} (~50%) after Ch-T modification of *h*Slo1 + *m*β1 in 2.1 μM $[Ca^{2+}]_i$ indicates that Ca^{2+} makes a smaller free energy contribution to overall channel opening after oxidation (Fig. 8 A, inset).

Biophysical Model Simulation

The functional effects of oxidation by Ch-T of the *h*Slo1 + β1 complex in the virtual absence of Ca^{2+} may be interpreted using the HCA allosteric gating model (Fig. 9 A; Horrigan et al., 1999) as performed for the *h*Slo1 channel without β1 (Tang et al., 2001). The voltage dependence of *h*Slo1 alone shifts by −30 mV, and the deactivation time course slows after oxidation by Ch-T. To account for these alterations, Tang et al. (2001) increased the value of the strongly voltage-dependent parameter α(0), which may correspond to movement of the voltage sensor (Horrigan et al., 1999), by 2.3-fold and decreased the rate constant of the closing transition dominant at negative voltages (γ_0) by 60% (Fig. 9 B; Tang et al., 2001, Fig. 14). We simulated the potentiated effects of Ch-T treatment in the presence of β1 in the following manner. First, the value of α(0) is further increased (about twofold) to account for the larger shift, −75 mV, of the G-V curve (Fig. 9 B). Second, the closing rate constant γ_0 decreases by an additional 40% to account for the greater slowing of the tail kinetics. Third, in addition to the two quantitative changes listed, the rate constant for the

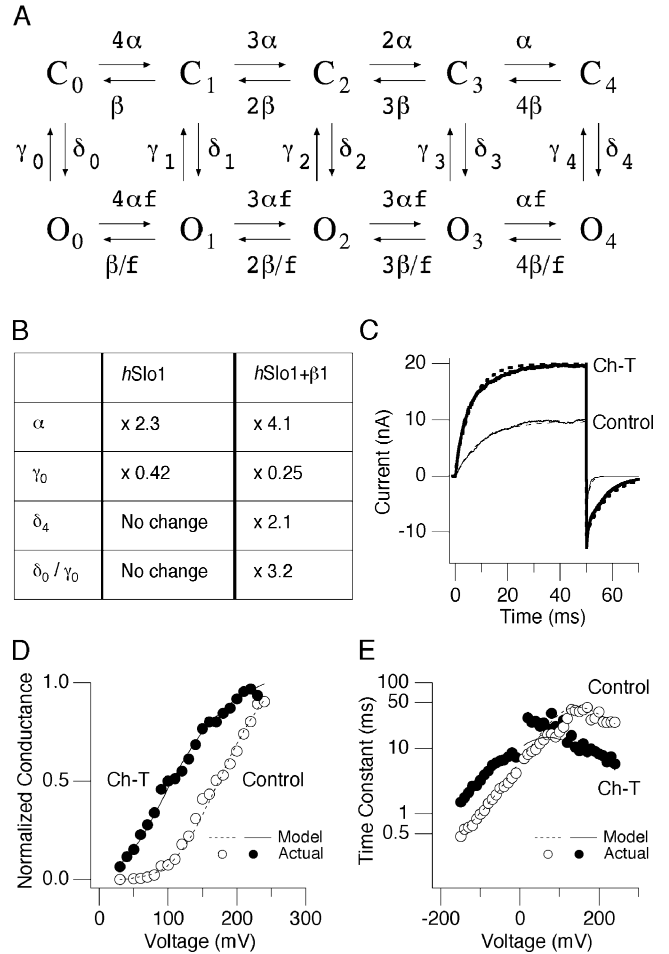

FIGURE 9. Simulation of oxidation by Ch-T on *h*Slo1 + β1 function based on the HCA model. (A) The HCA allosteric gating model (Horrigan et al., 1999). The most probable opening of the channel at strongly depolarized voltages involves transitions from C_0 to C_1, C_2, C_3, C_4, and then O_4. Likewise, channel closing at negative voltages entails transitions from O_4 to O_3, O_2, O_1, O_0, and then C_0. (B) Adjustments in average parameter values from the HCA model required to simulate the effect of modification by Ch-T on *h*Slo1 (Tang et al., 2001) or *h*Slo1 + β1 function. HCA model values are as follows: $\alpha(0) = 1{,}500\ s^{-1}$, $\beta(0) = 35{,}370\ s^{-1}$, $\delta_0(0) = 0.007\ s^{-1}$, $\delta_1(0) = 0.154\ s^{-1}$, $\delta_2(0) = 3.39\ s^{-1}$, $\delta_3(0) = 52\ s^{-1}$, $\delta_4(0) = 65\ s^{-1}$, $D = 22$, $f = D^{0.5}$, and $L(0) = \delta_0(0)/\gamma_0(0) = 2 \times 10^{-6}$. $L(0)$ represents the open-to-closed equilibrium constant in the absence of an applied voltage. (C) Experimental *h*Slo1 + *m*β1 currents (continuous sweeps) recorded at 160 mV before (thin) and after (thick) oxidation by Ch-T and simulated currents (dashed lines) from the HCA model adjusted for the effect of Ch-T in the presence of β1. (D) G-V curves from a patch containing *h*Slo1 + *m*β1 before (open circles) and after (closed circles) treatment with Ch-T. Data simulated from the *h*Slo1 + β1 model before (dotted line) and after (continuous line) Ch-T are superimposed. (E) Activation/deactivation time constants. Symbols are the same as in D.

opening transition dominant at positive voltages (δ_4) is increased by 2.1-fold to account for the unique acceleration of the activation kinetics observed in *h*Slo1 + β1 but not in *h*Slo1 alone. Simulated data produced from

this model that account for the effect of Ch-T on *h*Slo1 function with β1 present match the experimental data (Fig. 9, C–E).

DISCUSSION

Methionine Oxidation Leads to Distinct Alterations in hSlo1 + β1 Function

Coexpression of β1 with *h*Slo1 is known to affect the activation/deactivation kinetics and apparent Ca^{2+} sensitivity of the channel (Orio et al., 2002). Here, we have demonstrated that oxidation of *h*Slo1 in the presence of the auxiliary subunit β1 leads to functional effects clearly distinguishable from those observed with *h*Slo1 alone. Oxidation of *h*Slo1 promoted by Ch-T causes a leftward shift of the G-V curve by ∼30 mV. However, this hyperpolarizing shift is more than twice as great (∼75 mV) in the presence of β1. Furthermore, the Ch-T–induced slowing of *h*Slo1 deactivation is even more dramatic with β1 present. In addition, β1 confers a novel effect of oxidation not observed with *h*Slo1 alone; modification by Ch-T leads to the distinct acceleration of *h*Slo1 activation evident at each depolarized voltage only with the inclusion of β1 into the channel complex. These unique features of oxidative modification in the presence of the β1 subunit overall cannot be accounted for by a difference in the modification rate as compared with *h*Slo1 alone or a simple voltage-dependent shift in the open probability and activation/deactivation kinetics.

Role of Cysteine and Methionine Residues in β1

Because Ch-T preferentially oxidizes methionine residues under physiological conditions (Levine et al., 1996), methionine is implicated as the main target of oxidation by Ch-T that is responsible for the observed functional alterations in both *h*Slo1 and *h*Slo1 + β1. However, protein-modifying agents may not be perfectly specific for one particular amino acid. In fact, both cysteine and methionine are possible physiological targets of Ch-T. To determine if cysteine oxidation plays a role in the Ch-T effect on *h*Slo1 alone, Tang et al. (2001) previously showed that cysteine-specific reagents (5,5′-dithio-bis (2-nitrobenzoic acid), methanethiosulfonate ethylammonium, and *p*-chloromercuribenzoic acid) actually decreased channel activity, thereby demonstrating that cysteine oxidation has opposite effects on channel function than methionine oxidation. Furthermore, the Ch-T–induced potentiation was maintained in *h*Slo1 mutants that lacked most of the cysteine residues within the channel. Finally, peptide methionine sulfoxide reductase, an enzyme that catalyzes the reduction of met-O (Weissbach et al., 2002), partially reversed the effect of Ch-T treatment. Therefore, the functional alterations caused by Ch-T were attributed to methionine oxidation within *h*Slo1.

Cysteine residues within β1 are not required for typical regulation of *h*Slo1 kinetics or the enhanced effects on channel function after oxidation. The *b*β1 subunit devoid of any cysteine residues behaves much like wild-type *b*β1 in terms of slowing *h*Slo1 activation and deactivation. Furthermore, after oxidation by Ch-T, the cysteine mutations still permit the significantly larger $\Delta V_{0.5}$ value, the slower deactivation kinetics and the accelerated channel activation similar to those observed with wild-type *b*β1. These results indicate that cysteine is not the likely Ch-T target responsible for causing the functional changes after oxidation.

Similar to the *b*β1 cysteine mutant, the *m*β1 methionine mutants regulate *h*Slo1 kinetics much like wild-type β1. Moreover, all *m*β1 methionine mutants including the triple mutant maintain the dramatic shift of the G-V curve toward the hyperpolarizing direction and the enhanced slowing of channel deactivation after oxidation by Ch-T. Evaluation of the role of the initial β1 methionine residue (M1) is not straightforward. However, its contribution to the enhanced oxidative regulation of *h*Slo1, although a possibility, is unlikely due to potential removal by posttranslational processing of the mature protein (Creighton, 1993). Therefore, the presence of the β1 subunit provides the possibility to amplify the functional effects of methionine oxidation within the *h*Slo1 pore-forming subunit with regard to channel open probability and deactivation.

β1 M177 Involvement in the Functional Interaction with Slo1

Although the enhanced shift of the G-V curve and slowing of *h*Slo1 deactivation does not require cysteine or methionine residues within β1, the effect of oxidation on *h*Slo1 activation critically depends on M177 in TM2 of *m*β1. In the control condition, only M177L *m*β1 causes a significant difference in the channel activation time course. Furthermore, the M177L mutation eliminates the oxidative sensitivity of channel activation typically observed with β1 present. Thus, M177 controls the *h*Slo1 activation kinetics at very positive voltages, which is described by the rate constant δ_4 in the HCA model (Fig. 9), and oxidation of M177 to met-O most likely mediates the Ch-T–induced acceleration of activation kinetics. However, the possibility that the M177L mutation hinders the access of Ch-T to its target elsewhere cannot be completely eliminated.

The mutant-specific effect on channel activation suggests a partial uncoupling of *h*Slo1 and β1 because of mutation or oxidation at the M177 position. Because the activation kinetics of *h*Slo1 is faster without β1, oxidation of *h*Slo1 + β1 may cause channel activation to be more like *h*Slo1 alone by removal of the β1 influ-

ence. The hydrophobic leucine mutation at M177 mimics the presence of met-O at that location because the control activation kinetics of *h*Slo1 + M177L *m*β1 resembles that of oxidized *h*Slo1+ wild-type *m*β1. Indeed, an increase in surface hydrophobicity, while somewhat paradoxical, has been shown after oxidation of methionine residues within the enzyme glutamine synthetase (Levine et al., 1996). Perhaps oxidation of M177 to met-O, whereby acting as the sensor or switch, partially disrupts an interaction between the β1 subunit and the structural elements in or near the RCK (regulator of K^+ conductance) domains within *h*Slo1 that are specifically responsible for controlling activation kinetics. Similar to the effect of β1 M177 on channel activation, other residues within different β subunits influence functional coupling of the auxiliary subunit and *h*Slo1. For example, the phosphorylation states of T11/S17 in the cytoplasmic NH_2 terminus and S210 in the cytoplasmic COOH terminus within β4 affect the functional coupling between *h*Slo1 and β4, as determined by changes in channel voltage dependence and activation/deactivation kinetics specific to modification of the different residues (Jin et al., 2002).

Physiological Implications

As found with *h*Slo1 alone, the effect of methionine oxidation on *h*Slo1 function in the presence of β1 is sensitive to $[Ca^{2+}]_i$. In the virtual absence of $[Ca^{2+}]_i$, *h*Slo1 + *m*β1 displays a hyperpolarizing shift of $V_{0.5}$ that is twice as great as *h*Slo1 alone after oxidation by Ch-T. This Ch-T–induced shift resembles the presence of ~0.4 μM $[Ca^{2+}]_i$ (Cox and Aldrich, 2000). The oxidized channel complex can open in the physiological voltage range (<50 mV) without $[Ca^{2+}]_i$ as further evidenced by the increase in open probability observed at −40 mV. An increase in channel open probability at low $[Ca^{2+}]_i$ could have an impact on resting BK_{Ca} channel activity in smooth muscle cells, thereby influencing vascular tone. Because BK_{Ca} channels crucially shape the action potential posthyperpolarization phase in certain cell types, this increase in channel open probability may prevent unregulated neuronal firing (Lancaster and Nicoll, 1987; Storm, 1987; Marsh and Brown, 1991; Zhang and McBain, 1995; Pedarzani et al., 2000; Faber and Sah, 2002; Edgerton and Reinhart, 2003).

The concept that the binding of Ca^{2+} performs mechanical work to open the Slo1 channel (Jiang et al., 2002) has been further developed into a spring-based gating mechanism in which the diameter of the gating ring, formed by the RCK domains from each Slo1 subunit, expands upon Ca^{2+} binding, thereby generating an active force that pulls the S6-RCK1 linker regions that act as the springs, thus opening the channel gates (Niu et al., 2004). This proposed gating process might be similarly affected by methionine oxidation, which biases the open channel state. In the absence of $[Ca^{2+}]_i$, oxidation of methionine residues to met-O within the *h*Slo1 pore-forming subunit may likewise affect the structure or position of the gating ring ultimately influencing gating of the channel. The lack of a hyperpolarizing shift of $V_{0.5}$ in response to modification by Ch-T at high $[Ca^{2+}]_i$ indicates that the effects of Ca^{2+} and methionine oxidation on channel gating are not additive and may in fact operate on the same effectors. In the case of the *h*Slo1 + β1 channel complex, the presence of β1 may cause a unique conformational change in *h*Slo1, such that additional methionine residues in *h*Slo1 are exposed and able to react with Ch-T, thereby accounting for the enhanced functional effects of oxidation. However, the similarity in the modification time courses of *h*Slo1 and *h*Slo1 + *m*β1 argues against this possibility.

Modification of ion channels by ROS/RNS during oxidative stress could alter channel function and eventually disrupt normal $[Ca^{2+}]_i$ and other homeostatic parameters (Kourie, 1998). Potential consequences of oxidative stress include accelerated aging (Hensley and Floyd, 2002), as well as pathophysiological conditions such as various neurodegenerative disorders (Coyle and Puttfarcken, 1993) and ischemia-reperfusion injury after stroke (Babbs, 1988; Rubanyi, 1988). However, certain ion channel modifications by ROS/RNS may serve as compensatory mechanisms to oxidative assault. One such example involves the mitochondrial ATP-sensitive K^+ channel ($mitoK_{ATP}$) that is activated by ROS during initial, mild ischemia; as a result, the heart is preconditioned to future ischemic attacks and infarctions (Szewczyk and Marban, 1999; Grover and Garlid, 2000; Zhang et al., 2001). Much like the $mitoK_{ATP}$ channel, the BK_{Ca} channel clearly represents a prime candidate for aiding in the recovery from ROS/RNS attack given its localization in brain and smooth muscle, as well as the documented oxidation-related alteration of its function (DiChiara and Reinhart, 1997; Sobey et al., 1997; Wang and Wu, 1997; Wang et al., 1997; Barlow et al., 2000; Gong et al., 2000; Soh et al., 2001; Tang et al., 2001, 2004; Brakemeier et al., 2003). Whether the BK_{Ca} channel contributes to the progression of oxidative stress-related conditions or instead serves a more compensatory role—such as maintaining resting membrane potential if $[Ca^{2+}]_i$ is disrupted—remains to be determined.

In summary, we showed that in the virtual absence of Ca^{2+}, methionine oxidation by Ch-T dramatically alters *h*Slo1 function with the association of the β1 subunit. The presence of β1 as opposed to methionine and/or cysteine oxidation within this auxiliary subunit greatly amplifies the increase in channel open probability and the slowing of deactivation derived from oxidation of the *h*Slo1 pore-forming subunit. The target methionine

residues within *h*Slo1 are not yet known, but may be found in the S5/P/S6 segments (Tang et al., 2001) and/or the gating ring region (Niu et al., 2004). In contrast, M177 within β1 influences *h*Slo1 activation and most likely serves as the methionine target responsible for the acceleration in channel activation after methionine oxidation in the presence of the β1 subunit. Testing the oxidative effects with β subunits present provides more relevant results that can then be readily extended to physiological or pathophysiological conditions. Whether the effect of methionine oxidation on *h*Slo function in the presence of other β subunits (β2–4) also occurs remains to be determined, but β1 clearly facilitates unique modulation of channel function in the face of oxidation.

We thank Dr. D.R. Wassef and P. Rothenberg for help with mutant construction, Dr. R. Xu for cell culture, Dr. M.L. Garcia for the generous gift of the Cysless β1 mutant as well as helpful discussions, Dr. X.D. Tang for physiology discussions, and D. Armstrong and V.P. Santarelli for their views and advice.

This work was supported in part by grants from the National Institutes of Health (to L.C. Santarelli and T. Hoshi), Thüringer Ministerium für Wissenschaft B307-04004 (to S.H. Heinemann), and the National Natural Science Foundation of China (grant 30270351 to J. Chen).

Olaf S. Andersen served as editor.

Submitted: 7 July 2004
Accepted: 23 August 2004

REFERENCES

Amberg, G.C., and L.F. Santana. 2003. Downregulation of the BK channel β1 subunit in genetic hypertension. *Circ. Res.* 93:965–971.

Amberg, G.C., A.D. Bonev, C.F. Rossow, M.T. Nelson, and L.F. Santana. 2003. Modulation of the molecular composition of large conductance, Ca^{2+} activated K^+ channels in vascular smooth muscle during hypertension. *J. Clin. Invest.* 112:717–724.

Avdonin, V., and T. Hoshi. 2001. Modification of voltage-dependent gating of potassium channels by free form of tryptophan side chain. *Biophys. J.* 81:97–106.

Avdonin, V., X.D. Tang, and T. Hoshi. 2003. Stimulatory action of internal protons on Slo1 BK channels. *Biophys. J.* 84:2969–2980.

Babbs, C.F. 1988. Reperfusion injury of postischemic tissues. *Ann. Emerg. Med.* 17:1148–1157.

Barlow, R.S., A.M. El-Mowafy, and R.E. White. 2000. H_2O_2 opens BK_{Ca} channels via the PLA2-arachidonic acid signaling cascade in coronary artery smooth muscle. *Am. J. Physiol. Heart Circ. Physiol.* 279:H475–H483.

Brakemeier, S., I. Eichler, A. Knorr, T. Fassheber, R. Kohler, and J. Hoyer. 2003. Modulation of Ca^{2+}-activated K^+ channel in renal artery endothelium *in situ* by nitric oxide and reactive oxygen species. *Kidney Int.* 64:199–207.

Brenner, R., T.J. Jegla, A. Wickenden, Y. Liu, and R.W. Aldrich. 2000a. Cloning and functional characterization of novel large conductance calcium-activated potassium channel beta subunits, hKCNMB3 and hKCNMB4. *J. Biol. Chem.* 275:6453–6461.

Brenner, R., G.J. Perez, A.D. Bonev, D.M. Eckman, J.C. Kosek, S.W. Wiler, A.J. Patterson, M.T. Nelson, and R.W. Aldrich. 2000b. Vasoregulation by the β1 subunit of the calcium-activated potassium channel. *Nature.* 407:870–876.

Butterfield, D.A., B.J. Howard, and M.A. LaFontaine. 2001. Brain oxidative stress in animal models of accelerated aging and the age-related neurodegenerative disorders, Alzheimer's disease and Huntington's disease. *Curr. Med. Chem.* 8:815–828.

Ciorba, M.A., S.H. Heinemann, H. Weissbach, N. Brot, and T. Hoshi. 1997. Modulation of potassium channel function by methionine oxidation and reduction. *Proc. Natl. Acad. Sci. USA.* 94:9932–9937.

Cox, D.H., and R.W. Aldrich. 2000. Role of the β1 subunit in large-conductance Ca^{2+}-activated K^+ channel gating energetics. Mechanisms of enhanced Ca^{2+} sensitivity. *J. Gen. Physiol.* 116:411–432.

Coyle, J.T., and P. Puttfarcken. 1993. Oxidative stress, glutamate, and neurodegenerative disorders. *Science.* 262:689–695.

Creighton, T.E. 1993. Proteins: Structures and Molecular Properties. 2nd edition. W.H. Freeman Publishers, New York. 507 pp.

Cui, J., and R.W. Aldrich. 2000. Allosteric linkage between voltage and Ca^{2+}-dependent activation of BK-type mslo1 K^+ channels. *Biochemistry.* 39:15612–15619.

DiChiara, T.J., and P.H. Reinhart. 1997. Redox modulation of *hslo* Ca^{2+}-activated K^+ channels. *J. Neurosci.* 17:4942–4955.

Dworetzky, S.I., J.T. Trojnacki, and V.K. Gribkoff. 1994. Cloning and expression of a human large-conductance calcium-activated potassium channel. *Brain Res. Mol. Brain Res.* 27:189–193.

Edgerton, J.R., and P.H. Reinhart. 2003. Distinct contributions of small and large conductance Ca^{2+}-activated K^+ channels to rat Purkinje neuron function. *J. Physiol.* 548:53–69.

Faber, E.S., and P. Sah. 2002. Physiological role of calcium-activated potassium currents in the rat lateral amygdala. *J. Neurosci.* 22:1618–1628.

Fernandez-Fernandez, J.M., M. Tomas, E. Vazquez, P. Orio, R. Latorre, M. Senti, J. Marrugat, and M.A. Valverde. 2004. Gain-of-function mutation in the KCNMB1 potassium channel subunit is associated with low prevalence of diastolic hypertension. *J. Clin. Invest.* 113:1032–1039.

Garcia-Calvo, M., H.G. Knaus, O.B. McManus, K.M. Giangiacomo, G.J. Kaczorowski, and M.L. Garcia. 1994. Purification and reconstitution of the high-conductance, calcium-activated potassium channel from tracheal smooth muscle. *J. Biol. Chem.* 269:676–682.

Giangiacomo, K.M., M. Garcia-Calvo, K. Hans-Gunther, T.J. Mullmann, M.L. Garcia, and O. McManus. 1995. Functional reconstitution of the large-conductance, calcium-activated potassium channel purified from bovine aortic smooth muscle. *Biochemistry.* 34:15849–15862.

Gollasch, M., J. Tank, F.C. Luft, J. Jordan, P. Maass, C. Krasko, A.M. Sharma, A. Busjahn, and S. Bahring. 2002. The BK channel β1 subunit gene is associated with human baroreflex and blood pressure regulation. *J. Hypertens.* 20:927–933.

Gong, L., T.M. Gao, H. Huang, and Z. Tong. 2000. Redox modulation of large conductance calcium-activated potassium channels in CA1 pyramidal neurons from adult rat hippocampus. *Neurosci. Lett.* 286:191–194.

Grover, G.J., and K.D. Garlid. 2000. ATP-sensitive potassium channels: a review of their cardioprotective pharmacology. *J. Mol. Cell. Cardiol.* 32:677–695.

Hanner, M., R. Vianna-Jorge, A. Kamassah, W.A. Schmalhofer, H.G. Knaus, G.J. Kaczorowski, and M.L. Garcia. 1998. The β subunit of the high conductance calcium-activated potassium channel. Identification of residues involved in charybdotoxin binding. *J. Biol. Chem.* 273:16289–16296.

Hensley, K., and R.A. Floyd. 2002. Reactive oxygen species and protein oxidation in aging: a look back, a look ahead. *Arch. Biochem. Biophys.* 397:377–383.

Horrigan, F.T., and R.W. Aldrich. 1999. Allosteric voltage gating of potassium channels II. mslo channel gating charge movement in

the absence of Ca^{2+}. *J. Gen. Physiol.* 114:305–336.

Horrigan, F.T., J. Cui, and R.W. Aldrich. 1999. Allosteric voltage gating of potassium channels I. mslo ionic currents in the absence of Ca^{2+}. *J. Gen. Physiol.* 114:277–304.

Jaggar, J.H., V.A. Porter, W.J. Lederer, and M.T. Nelson. 2000. Calcium sparks in smooth muscle. *Am. J. Physiol. Cell Physiol.* 278: C235–C256.

Jiang, Y., A. Lee, J. Chen, M. Cadene, B.T. Chait, and R. MacKinnon. 2002. Crystal structure and mechanism of a calcium-gated potassium channel. *Nature.* 417:515–522.

Jiang, Z., M. Wallner, P. Meera, and L. Toro. 1999. Human and rodent MaxiK channel β-subunit genes: cloning and characterization. *Genomics.* 55:57–67.

Jin, P., T.M. Weiger, Y. Wu, and I.B. Levitan. 2002. Phosphorylation-dependent functional coupling of h*Slo* calcium-dependent potassium channel and its hβ4 subunit. *J. Biol. Chem.* 277:10014–10020.

Knaus, H.G., K. Folander, M. Garcia-Calvo, M.L. Garcia, G.J. Kaczorowski, M. Smith, and R. Swanson. 1994. Primary sequence and immunological characterization of β-subunit of high conductance Ca^{2+}-activated K^+ channel from smooth muscle. *J. Biol. Chem.* 269:17274–17278.

Knight, J.A. 1997. Reactive oxygen species and the neurodegenerative disorders. *Ann. Clin. Lab. Sci.* 27:11–25.

Kourie, J.I. 1998. Interaction of reactive oxygen species with ion transport mechanisms. *Am. J. Physiol.* 275:C1–C24.

Lancaster, B., and R.A. Nicoll. 1987. Properties of two calcium-activated hyperpolarizations in rat hippocampal neurones. *J. Physiol.* 389:187–203.

Levine, R.L., L. Mosoni, B.S. Berlett, and E.R. Stadtman. 1996. Methionine residues as endogenous antioxidants in proteins. *Proc. Natl. Acad. Sci. USA.* 93:15036–15040.

Markesbery, W.R. 1997. Oxidative stress hypothesis in Alzheimer's disease. *Free Radic. Biol. Med.* 23:134–147.

Marsh, S.J., and D.A. Brown. 1991. Potassium currents contributing to action potential repolarization in dissociated cultured rat superior cervical sympathetic neurones. *Neurosci. Lett.* 133:298–302.

McManus, O.B., L.M. Helms, L. Pallanck, B. Ganetzky, R. Swanson, and R.J. Leonard. 1995. Functional role of the β subunit of high conductance calcium-activated potassium channels. *Neuron.* 14: 645–650.

Meera, P., M. Wallner, Z. Jiang, and L. Toro. 1996. A calcium switch for the functional coupling between α (hslo) and β subunits ($K_{V,Ca}$ β) of maxi K channels. *FEBS Lett.* 382:84–88.

Meera, P., M. Wallner, M. Song, and L. Toro. 1997. Large conductance voltage- and calcium-dependent K^+ channel, a distinct member of voltage-dependent ion channels with seven N-terminal transmembrane segments (S0-S6), an extracellular N terminus, and an intracellular (S9-S10) C terminus. *Proc. Natl. Acad. Sci. USA.* 94:14066–14071.

Meredith, A.L., K.S. Thorneloe, M.E. Werner, M.T. Nelson, and R.W. Aldrich. 2004. Overactive bladder and incontinence in the absence of the BK large conductance Ca^{2+}-activated K^+ channel. *J. Biol. Chem.* 10.1074/jbc.M405621200.

Nelson, M.T., H. Cheng, M. Rubart, L.F. Santana, A.D. Bonev, H.J. Knot, and W.J. Lederer. 1995. Relaxation of arterial smooth muscle by calcium sparks. *Science.* 270:633–637.

Nimigean, C.M., and K.L. Magleby. 1999. The β subunit increases the Ca^{2+} sensitivity of large conductance Ca^{2+}-activated potassium channels by retaining the gating in the bursting states. *J. Gen. Physiol.* 113:425–440.

Nimigean, C.M., and K.M. Magleby. 2000. Functional coupling of the β1 subunit to the large conductance Ca^{2+}-activated K^+ channel in the absence of Ca^{2+}: increased Ca^{2+} sensitivity from a Ca^{2+}-independent mechanism. *J. Gen. Physiol.* 115:719–736.

Niu, X., X. Qian, and K.L. Magleby. 2004. Linker-gating ring complex as passive spring and Ca^{2+}-dependent machine for a voltage- and Ca^{2+}-activated potassium channel. *Neuron.* 42:745–756.

Orio, P., P. Rojas, G. Ferreira, and R. Latorre. 2002. New disguises for an old channel: MaxiK channel β-subunits. *News Physiol. Sci.* 17:156–161.

Pallanck, L., and B. Ganetzky. 1994. Cloning and characterization of human and mouse homologs of the *Drosophila* calcium-activated potassium channel gene, slowpoke. *Hum. Mol. Genet.* 3:1239–1243.

Patterson, A.J., J. Henrie-Olson, and R. Brenner. 2002. Vasoregulation at the molecular level: a role for the β1 subunit of the calcium-activated potassium (BK) channel. *Trends Cardiovasc. Med.* 12:78–82.

Pedarzani, P., A. Kulik, M. Muller, K. Ballanyi, and M. Stocker. 2000. Molecular determinants of Ca^{2+}-dependent K^+ channel function in rat dorsal vagal neurones. *J. Physiol.* 527:283–290.

Pluger, S., J. Faulhaber, M. Furstenau, M. Lohn, R. Waldschutz, M. Gollasch, H. Haller, F.C. Luft, H. Ehmke, and O. Pongs. 2000. Mice with disrupted BK channel β1 subunit gene feature abnormal Ca^{2+} Spark/STOC coupling and elevated blood pressure. *Circ. Res.* 87:E53–E60.

Qian, X., and K.L. Magleby. 2003. β1 subunits facilitate gating of BK channels by acting through the Ca^{2+}, but not the Mg^{2+}, activating mechanisms. *Proc. Natl. Acad. Sci. USA.* 100:10061–10066.

Rubanyi, G.M. 1988. Vascular effects of oxygen-derived free radicals. *Free Radic. Biol. Med.* 4:107–120.

Sausbier, M., H. Hu, C. Arntz, S. Feil, S. Kamm, H. Adelsberger, U. Sausbier, C.A. Sailer, R. Feil, F. Hofmann, et al. 2004. Cerebellar ataxia and Purkinje cell dysfunction caused by Ca^{2+}-activated K^+ channel deficiency. *Proc. Natl. Acad. Sci. USA.* 101:9474–9478.

Sobey, C.G., D.D. Heistad, and F.M. Faraci. 1997. Mechanisms of bradykinin-induced cerebral vasodilatation in rats. Evidence that reactive oxygen species activate K^+ channels. *Stroke.* 28:2290–2294.

Soh, H., W. Jung, D.Y. Uhm, and S. Chung. 2001. Modulation of large conductance calcium-activated potassium channels from rat hippocampal neurons by glutathione. *Neurosci. Lett.* 298:115–118.

Soto, M.A., C. Gonzalez, E. Lissi, C. Vergara, and R. Latorre. 2002. Ca^{2+}-activated K^+ channel inhibition by reactive oxygen species. *Am. J. Physiol. Cell Physiol.* 282:C461–C471.

Storm, J.F. 1987. Action potential repolarization and a fast after-hyperpolarization in rat hippocampal pyramidal cells. *J. Physiol.* 385:733–759.

Szewczyk, A., and E. Marban. 1999. Mitochondria: a new target for K channel openers? *Trends Pharmacol. Sci.* 20:157–161.

Tanaka, Y., P. Meera, M. Song, H.G. Knaus, and L. Toro. 1997. Molecular constituents of maxi K_{Ca} channels in human coronary smooth muscle: predominant α + β subunit complexes. *J. Physiol.* 502:545–557.

Tang, X.D., H. Daggett, M. Hanner, M.L. Garcia, O.B. McManus, N. Brot, H. Weissbach, S.H. Heinemann, and T. Hoshi. 2001. Oxidative regulation of large conductance calcium-activated potassium channels. *J. Gen. Physiol.* 117:253–274.

Tang, X.D., M.L. Garcia, S.H. Heinemann, and T. Hoshi. 2004. Reactive oxygen species impair Slo1 BK channel function by altering cysteine-mediated calcium sensing. *Nat. Struct. Mol. Biol.* 11: 171–178.

Taniyama, Y., and K.K. Griendling. 2003. Reactive oxygen species in the vasculature: molecular and cellular mechanisms. *Hypertension.* 42:1075–1081.

Tseng-Crank, J., C.D. Foster, J.D. Krause, R. Mertz, N. Godinot, T.J. DiChiara, and P.H. Reinhart. 1994. Cloning, expression, and distribution of functionally distinct Ca^{2+}- activated K^+ channel iso-

forms from human brain. *Neuron.* 13:1315–1330.

Tseng-Crank, J., N. Godinot, T.E. Johansen, P.K. Ahring, D. Strobaek, R. Mertz, C.D. Foster, S.P. Olesen, and P.H. Reinhart. 1996. Cloning, expression, and distribution of a Ca^{2+}-activated K^+ channel β-subunit from human brain. *Proc. Natl. Acad. Sci. USA.* 93:9200–9205.

Uebele, V.N., A. Lagrutta, T. Wade, D.J. Figueroa, Y. Liu, E. McKenna, C.P. Austin, P.B. Bennett, and R. Swanson. 2000. Cloning and functional expression of two families of β-subunits of the large conductance calcium-activated K^+ channel. *J. Biol. Chem.* 275:23211–23218.

Vogalis, F., T. Vincent, I. Qureshi, F. Schmalz, M.W. Ward, K.M. Sanders, and B. Horowitz. 1996. Cloning and expression of the large-conductance Ca^{2+}-activated K^+ channel from colonic smooth muscle. *Am. J. Physiol.* 271:G629–G639.

Wallner, M., P. Meera, M. Ottolia, G.J. Kaczorowski, R. Latorre, M.L. Garcia, E. Stefani, and L. Toro. 1995. Characterization of and modulation by a β-subunit of a human maxi K_{Ca} channel cloned from myometrium. *Receptors Channels.* 3:185–199.

Wallner, M., P. Meera, and L. Toro. 1996. Determinant for β-subunit regulation in high-conductance voltage-activated and Ca^{2+}-sensitive K^+ channels: an additional transmembrane region at the N terminus. *Proc. Natl. Acad. Sci. USA.* 93:14922–14927.

Wang, R., and L. Wu. 1997. The chemical modification of K_{Ca} channels by carbon monoxide in vascular smooth muscle cells. *J. Biol. Chem.* 272:8222–8226.

Wang, Z.W., M. Nara, Y.X. Wang, and M.I. Kotlikoff. 1997. Redox regulation of large conductance Ca^{2+}-activated K^+ channels in smooth muscle cells. *J. Gen. Physiol.* 110:35–44.

Wanner, S.G., R.O. Koch, A. Koschak, M. Trieb, M.L. Garcia, G.J. Kaczorowski, and H.G. Knaus. 1999. High-conductance calcium-activated potassium channels in rat brain: pharmacology, distribution, and subunit composition. *Biochemistry.* 38:5392–5400.

Weiger, T.M., A. Hermann, and I.B. Levitan. 2002. Modulation of calcium-activated potassium channels. *J. Comp. Physiol. A Neuroethol. Sens Neural. Behav. Physiol.* 188:79–87.

Weiger, T.M., M.H. Holmqvist, I.B. Levitan, F.T. Clark, S. Sprague, W.J. Huang, P. Ge, C. Wang, D. Lawson, M.E. Jurman, et al. 2000. A novel nervous system β subunit that downregulates human large conductance calcium-dependent potassium channels. *J. Neurosci.* 20:3563–3570.

Weissbach, H., F. Etienne, T. Hoshi, S.H. Heinemann, W.T. Lowther, B. Matthews, G. St. John, C. Nathan, and N. Brot. 2002. Peptide methionine sulfoxide reductase: structure, mechanism of action, and biological function. *Arch. Biochem. Biophys.* 397:172–178.

Xia, X.M., J.P. Ding, and C.J. Lingle. 1999. Molecular basis for the inactivation of Ca^{2+}- and voltage-dependent BK channels in adrenal chromaffin cells and rat insulinoma tumor cells. *J. Neurosci.* 19:5255–5264.

Zhang, D.X., Y.F. Chen, W.B. Campbell, A.P. Zou, G.J. Gross, and P.L. Li. 2001. Characteristics and superoxide-induced activation of reconstituted myocardial mitochondrial ATP-sensitive potassium channels. *Circ. Res.* 89:1177–1183.

Zhang, L., and C.J. McBain. 1995. Potassium conductances underlying repolarization and after-hyperpolarization in rat CA1 hippocampal interneurones. *J. Physiol.* 488:661–672.